

## **2. Characterisation techniques**



## **2. CHARACTERISATION TECHNIQUES**

The aim of this section is to facilitate the comprehension of the work by an unexperienced reader in structural characterisation and, in some way, to include a general description of a group of basic structural characterisation techniques in a clear way. For that, the principles in which the different techniques are based are presented. Additionally, the instrumentation used in each case is basically described, without entering in any case in great detail. For a reader interested in more details, a group of additional readings have been included. Thus, references [138-140] are for XRD, [141-148] for Raman and IR, [148-150] for XPS, [151-154] for TEM, [155-157] for ICP-OES, and [158-160] for SPM techniques.

### **2.1. X-Ray Diffraction**

One of the phenomena of interaction of X-rays with crystalline matter is its diffraction, produced by the reticular planes that form the atoms of the crystal. A crystal diffracts an X-ray beam passing through it to produce beams at specific angles depending on the X-ray wavelength, the crystal orientation and the structure of the crystal.

In the macroscopic version of X-ray diffraction, a certain wavelength of radiation will constructively interfere when partially reflected between surfaces (i.e., the atomic planes) that produce a path difference equal to an integral number of wavelengths. This condition is described by the Bragg law:

$$2d \sin \theta = n\lambda$$

where  $n$  is an integer,  $\lambda$  is the wavelength of the radiation,  $d$  is the spacing between surfaces and  $\theta$  is the angle between the radiation and the surfaces. This relation demonstrates that interference effects are observable only when radiation interacts with physical dimensions that are approximately the same size as the wavelength of the radiation. Since the distances between atoms or ions are on the order of  $10^{-10}$  m (1Å), diffraction methods require radiation in the X-ray region of the electromagnetic spectrum, or beams of electrons or neutrons with similar wavelength.

So, through X-ray spectra one can identify and analyse any crystalline matter. The degree of crystallinity or order will conditionate the quality of the obtained result. In order to do this, a diffractometer is needed. Basically, an X-ray diffractometer consists in an X-ray generator, a goniometer and sample holder and an X-ray detector, such as photographic film or a movable proportional counter. The most usually employed instrument to generate X-rays are X-ray tubes, which generate X-rays by bombarding a metal target with high energy (10-100keV) electrons that knock out core electrons. Thus, an electron in an outer shell fills the hole in the inner shell and emits an X-ray photon. Two common targets are Mo and Cu, which have strong  $K_{\alpha}$  X-ray emissions at 0.71073 and 1.5418Å, respectively. Apart from the main line, other accompanying lines appear, which have to be eliminated in order to facilitate the interpretation of the spectra. These are partially suppressed by using crystal monochromators.

The most interesting X-ray diffraction techniques for this work are those related to the analysis of polycrystalline materials and mainly of powders. In this case the powder provides all the possible orientations of the small crystals giving rise to a large number of diffraction cones, each one corresponding to a family of planes satisfying the Bragg's law. For large grains, rings are discontinuous and formed by small spots. As the size of the grains diminishes, the spots are closer and for an optimum size a continuous ring is obtained, which is transferred into a peak when working with graphic registers or lines in a photographic register. For lower grain sizes the clarity of rings is lost again and wide peaks or bands appear. When the crystals are not randomly but preferentially oriented, the intensity of the different rings and along each ring is not uniform.

Experimental acquisition of powder patterns can be done by using powder cameras or powder diffractometers. The simplest instrument is a powder camera and many factors can contribute to the decision to select a camera technique rather than a powder diffractometer. These include the lack of adequate sample quantity, the desire of maximum resolution and the lower initial cost. Of the various camera types the Debye-Scherrer camera is the most usually used, probably because it is the simplest and easiest to use. In it, the sample itself can be packed in a glass capillary or, if very small, mounted on the tip of a glass rod or other rigid material using rubber cement or other permanent adhesive. The sample is placed at the camera centre and aligned to the main beam. The intensities of the diffracted beams are proportional to the crystalline sample volume irradiated by the beam. Thus, exposure times have to be increased as the sample size decreases. In the Debye-Scherrer powder camera the whole diffraction pattern is recorded simultaneously. Two factors contributing to the low resolution of the Debye-Scherrer camera types are the incident-beam divergence due to a collimator, which is typically designed to yield the narrowest beam with usable intensity, and the size of the capillary. Debye-Scherrer data are generally of significantly poorer quality than diffractometer data, mainly because the shapes of the lines (or peaks) are affected by both the adsorption of the specimen and the physical size of the specimen.

In powder diffractometers a photon detector replaces the photographic film (or some annular detector) used in cameras. Early designs were non-focusing systems that utilised X-ray tube spot foci and required relatively long data collection times, giving rather poor resolution. Actually the majority of commercially available powder diffractometers use the Bragg-Brentano parafocusing arrangement. A given instrument may provide a horizontal or vertical  $\theta/2\theta$  configuration or a vertical  $\theta/\theta$  configuration. In it, all the rays diffracted by suitably oriented crystallites in the specimen at an angle  $2\theta$  converge to a line at the receiving slit. The X-rays are detected by a radiation detector, usually a scintillation counter or a sealed gas proportional counter. The receiving slit assembly and the detector are coupled together and move around a circle in order to scan a range of  $2\theta$  (Bragg) angles. For  $\theta/2\theta$  scans, the goniometer rotates the specimen about the same axis as the detector but at half the rotational speed. The surface of the specimen thus remains tangential to the focusing circle. In addition to being a device that accurately sets the angles  $\theta$  and  $2\theta$ , the goniometer also acts as a support for all of the various slits and other components which make up the diffractometer. The purpose of parallel-plate collimators is to limit the axial divergence of the beam and hence partially control the shape of the diffracted line profile. It follows that the centre of the specimen surface must be on the axis of the goniometer and this axis must be also parallel to the axis of the line focus, divergence slit and receiving slit.

In general, the major problems involved with the use of powder cameras are relatively long exposure times, the need to work with dark room facilities and difficulties in obtaining statistically precise count data.

Perhaps the most routine use of diffraction data is for phase identification. Each crystalline powder gives a unique diffraction diagram, which is the basis for a qualitative analysis by X-ray diffraction. Identification is practically always accompanied by the systematic comparison of the obtained spectrum with a standard one (a pattern), taken from any X-ray powder data file catalogues, published by the American Society for Testing and Materials (JCPDS). The diffraction profiles of a mixture of crystalline specimens consist in spectra of each of the individual crystalline substances present, superposed. Moreover, an accurate analysis of phase transitions in SGS materials can be also carried out when analysing samples treated at different annealing temperatures or even performing in-situ XRD analysis.

Quantitative analysis of diffraction profiles can be diverse. We will describe briefly the measure of grain size in polycrystalline specimens that, as previously discussed, is a crucial parameter in SGS.

The determination of the size of the crystals in a powder can be carried out thanks to measurements that must be made on the profile of the diffraction peaks. One of the functions that best describes the powder diffraction profiles is the Voigt function. This consists in a convolution product of a Lorentzian and Gaussian function and allows to: 1) Model size (Lorentzian component) and strain (Gaussian component) line-broadening contributions simultaneously; 2) Separate instrumental and specimen contributions to the diffracted line profile. Instrumental broadening is due to causes such as slit widths, sample size, penetration in the sample, imperfect focusing, etc.

For simplicity, instead of a Voigt function one usually uses a pseudo-Voigt function. This approximates the Lorentzian/Gaussian convolution product by using the simple addition of the two functions using a mixing parameter,  $\eta$ , which varies the function from Lorentzian to Gaussian for  $\eta=1$  to  $\eta=0$  respectively:

$$I_{i,k} = \frac{2\sqrt{\ln 2}}{H_k} \exp\left(\frac{-4 \ln 2}{H_k^2} (2\theta_i - 2\theta_k)^2\right) \quad \text{Gaussian (G)}$$

$$I_{i,k} = \frac{2}{\pi H_k} \left(1 + \frac{4(\sqrt{2}-1)}{H_k^2} (2\theta_i - 2\theta_k)^2\right)^{-1} \quad \text{Lorentzian (L)}$$

$$I_{i,k} = \eta L_{i,k} + (1-\eta)G_{i,k} \quad \text{Pseudo-Voigt}$$

For one peak analysis the procedure consists in evaluate the integral widths for Gaussian and Lorentzian contributions and the shape factor.

In practice, however, if one can neglect the micro-strain effects, which in addition sometimes give rise to mistakes and incongruencies in the evaluation of grain size, the above formulation reduces to the well-known Scherrer formula. Scherrer showed that the

average dimension of the crystals that compose a crystalline powder is related with the profile of the peak by means of the equation:

$$D = \frac{K\lambda}{\beta \cos \theta}$$

where K is a proportionality constant approximately similar to the unit,  $\beta$  the FWHM of the peak in radians (theoretically corrected from the instrumental broadening), D the size of the crystal in the direction perpendicular to the reflecting planes and  $\lambda$  the wavelength of the X-rays used. This is the most usual and simple equation that allows to evaluate grain size.

## **2.2. Raman**

The energy of a molecule or ion consists in four components that for a first approximation can be treated separately: the translational energy, the rotational energy, the vibrational energy and the electronic energy. When the molecule is placed in an electromagnetic field, a transfer of energy from the field to the molecule will occur only when the difference in energy between two quantified states equals  $h\nu$ , being h the Planck's constant and  $\nu$  the frequency of light. Because rotational levels are relatively close to each other, transitions between these levels occur at low frequencies, appearing pure rotational spectra between  $1 \text{ cm}^{-1}$  and  $10^2 \text{ cm}^{-1}$  (ultraviolet and visible regions).

In what respects to the vibrational spectra, when a molecule has n atoms there are  $3n-6$  independent vibrations ( $3n$  degrees of freedom minus the three coordinates related to translational and rotational movement); for linear molecules  $3n-5$ . These so-called normal vibrations can be observed by different techniques but specially by infrared and Raman scattering. Both rotation and vibration of molecules are involved in the adsorption of infrared radiation, but since molecular rotation is not usually resolved in most infrared and Raman spectra, we will ignore this additional consideration.

Like IR spectroscopy, Raman is an invaluable technique for characterisation of materials. In the field of semiconductor characterisation, the use of Raman microscopes is now widespread because it offers a non-destructive and quantitative microanalysis of structures and electronic properties. Because of its higher resolution with respect to FTIR spectroscopy and its versatility and simplicity in terms of sample handling and the possibility of acquisition of the whole spectra ( $4000$  to  $10 \text{ cm}^{-1}$ ) with the same instrument, Raman, and specially micro-Raman spectroscopy has actually an increasing use versus other similar spectroscopic techniques. In particular, in addition to the well known application of identification of compounds, a large number of reported works rule for example on the characterisation of concentration and mobility of free carriers, characterisation of strain and crystal quality, determination of local crystal orientation, etc. It is worth to comment that while IR and Raman spectra analyse basically the same vibrational behaviour of the molecule they are not exact duplicates since the selection rules and relative band intensities differ in many cases.

Raman spectra originate in the electronic polarisation caused by UV or visible light. The mechanism by which the incident radiation interacts with the molecular vibrational energy levels has its origins in the general phenomenon of light scattering, in which the electromagnetic radiation interacts with a pulsating deformable (polarisable) electron

cloud, being this interaction modulated by the molecular vibrations, i.e., it depends on the chemical structure of the molecules responsible for the scattering.

If a molecule is irradiated by monochromatic light of frequency  $\nu$  having electric field strength  $E$ , because of the electronic polarisation induced in the molecules by this incident light, it presents an induced dipole moment  $p$  that, at low  $E$  values, can be expressed as:

$$p = \alpha E$$

where  $\alpha$  is the polarizability tensor.

In normal Raman scattering the polarizability tensor is symmetric ( $\alpha_{xy} = \alpha_{yx} = \alpha_{zy}$ ). In molecules  $\alpha$  is not constant since certain vibrations and rotations can cause  $\alpha$  to vary.

The dispersed radiation can be of three types: elastic scattering, known as Rayleigh scattering, that has the same wavelength as that of the source; anti-Stokes Raman scattering, which has a greater frequency; and Stokes Raman scattering, which has lower frequency. As the variation of the polarizability will be smaller than the polarizability itself, Raman scattering should be less intense than Rayleigh scattering, as it is the case. Concretely, Raman scattering is a factor  $10^{-3}$  to  $10^{-4}$  weaker than Rayleigh scattering, being needed a strong exciting source to observe the Raman scattering. The linear dependency of Raman scattering with the incident beam intensity and sample concentration is also deduced.

The intensity of a Raman band depends on the polarizability of the molecule, the source intensity, the concentration of active groups, and other factors. Without absorption, the intensity of the Raman emission rises with the fourth potence of the source frequency. The Raman intensities are directly proportional to the concentration of active species.

Since Raman lines represent frequency differences from the incident frequency, they are also called Raman shifts and are designated as  $\Delta\nu$  in  $\text{cm}^{-1}$ . They are independent of the excitation wavelength.

As a result, the anti-Stokes lines are weaker than the red shifted spectrum where they appear as Stokes lines. The ratio of the intensities of equivalent pairs of lines  $I_{\text{anti-Stokes}}/I_{\text{Stokes}}$  falls as the vibrational frequency increases, and decreases with temperature.

Basically two types of Raman equipment can be described: Macro and micro-Raman. The former has the advantage of higher illumination region over the sample, being ideal for liquids and powder samples, and the disadvantage of the difficulty in focusing the specimen. The equipment used for both methods is basically the same, only a conventional optical microscope being added for micro-Raman spectroscopy.

A typical current Raman spectrometer incorporates (fig.2.1):

- 1) The illumination source composed of an  $\text{Ar}^+$  ion laser emitting lines between 458 and 529 nm, sometimes coupled to a dye laser or a solid state titanium sapphire laser providing tuneable radiation between 600 nm and 900 nm.

- 2) A macrosample chamber and a classical optical microscope for microanalysis.
- 3) A dispersive system composed of a double monochromator and a spectrograph. The two monochromators can be used either in subtractive mode to provide a wide field to the spectrograph or in additive mode when higher resolution is required. The double monochromator has one or two slits in between the first and second stage monochromators.
- 4) The detection system, which includes a multichannel detector (a linear diode array) and a photomultiplier connected to a single photon counter.

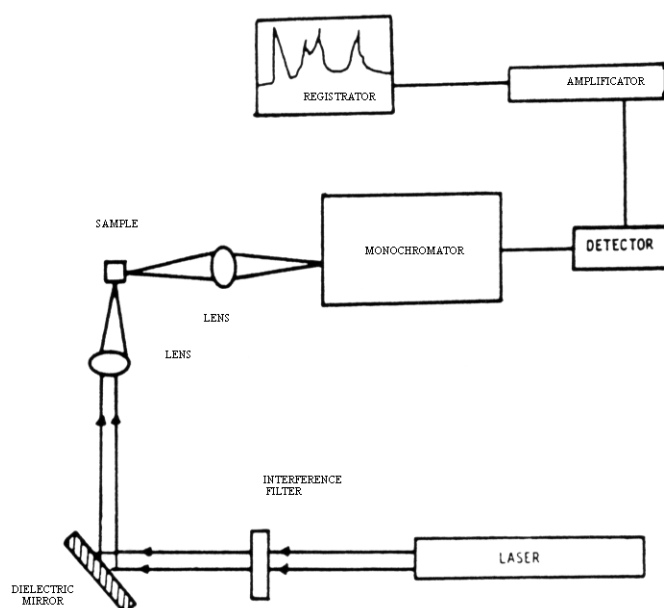


**Fig. 2.1.** *Schematic representation of a Raman spectrometer.*

Although three different types of sample illumination methods have been proposed for the measurement of local points and Raman mapping, being point illumination, line illumination and global illumination, the first is the most commonly employed. With point illumination the laser light is focussed on a sample surface by an objective lens and the scattered light is collected by the same objective. The spot size in the focal plane is diffraction limited. Although higher spatial resolution is obtained with this illumination method, heating or degradation of the samples by high density of laser powers can occur. Using a 100x objective with NA=0.95, the spot size in the sample is about 0.6  $\mu\text{m}$  for  $\lambda=457.9\text{nm}$ . This results in a very high power density in the specimen of the order of several  $\text{MW}/\text{cm}^2$ .

In this work, micro-Raman spectroscopy has been used not only for the identification of material structural phase and analysis of phase transitions, but also to determine when the catalytic species are placed inside the semiconductor lattice by analysing the Raman peaks shift.



### **2.3. Fourier Transform Infra Red**

Infrared spectroscopy is a very useful technique for characterisation of materials, not providing only information about the composition and the structure of molecules, but also morphological information. The advantages of infrared spectroscopy include wide applicability, nondestructiveness, measurement under ambient atmosphere and the capability of providing detailed structural information. Besides these intrinsic advantages (of the known as dispersive infrared spectroscopy), the more recent infrared spectroscopy by Fourier transform (FTIR) has additional merits such as: higher sensitivity, higher precision (improved frequency resolution and reproducibility), quickness of measurement and extensive data processing capability (as FTIR is a computer based technique, it allows storage of spectra and facilities for processing spectra).

IR spectra originate in transitions between two vibrational levels of a molecule in the electronic ground state and are usually observed as absorption spectra in the infrared region. For a molecule to present infrared absorption bands it is needed that it has a permanent dipole moment. When a molecule with at least one permanent dipole vibrates, this permanent dipole also vibrates and can interact with the oscillating electric field of incident infrared radiation. In order for this normal mode of vibration of the molecule to be infrared active, that is, to give rise to an observable infrared band, there must be a change in the dipole moment of the molecule during the course of the vibration.

Thus, if the vibrational frequency of the molecule, as determined by the force constant and reduced mass, equals the frequency of the electromagnetic radiation, then adsorption can take place. As the frequency of the electric field of the infrared radiation approaches the frequency of the oscillating bond dipole and the two oscillate at the same frequency and phase, the chemical bond can absorb the infrared photon and increase its vibrational quantum number by +1, or what is the same, increase its vibrational state to a higher level.

As a first approximation, the larger the strength of the bond the higher the frequency of the fundamental vibration. In the same way, the higher the masses of the atoms attached to the bond the lower the wavenumber of the fundamental vibration. As a general guide, the greater the number of groups of a particular type and more polar the bond, the more intense the band.

The infrared spectrum can be divided into two regions, one called the functional group region and the other the fingerprint region. The functional group region is generally considered to range from 4000 to 1500  $\text{cm}^{-1}$  and all frequencies below 1500  $\text{cm}^{-1}$  are considered characteristic of the fingerprint region. The fingerprint region involves molecular vibrations, usually bending motions, that are characteristic of the entire molecule or large fragments of the molecule. Thus these are used for identification. The functional group region tends to include motions, generally stretching vibrations, which are more localised and characteristic of the typical functional groups, found in organic molecules. While these bands are not very useful in confirming identity, they do provide some very useful information about the nature of the components that make up the molecule.

Basically an IR spectrometer is composed by the source, the monochromator and the receptor. The ideal IR source would be one that would give a continuous and high

radiant energy output over the entire IR region. The two sources in most common use are the Nernst Glower (heated up to 2200K) and the Globar (heated to about 1500K). In general, in all IR sources the radiant energy, which depends upon the temperature of the source, is low in the far infrared, and to obtain sufficient energy the slit width of the source has to be opened considerably with a corresponding decrease in resolution.

Between the source and the detector there must be some kind of device to analyse the radiation so that an intensity can be evaluated for each wavelength resolution element. There are two basic types, namely, monochromators, used in dispersive instruments, and interferometers used in Fourier transform instruments. In a monochromator, a prism or a diffraction grating is used, separating the components of polychromatic radiation. For spectroscopic work a prism must be transparent to the particular wavelength region of interest and the dispersion of the prism must be as large as possible.

The function of a grating, like that of a prism, is to provide monochromatic radiation from radiation composed of many wavelengths. A diffraction grating consists of a number of equally spaced slits, which diffract light by interference. The theoretical resolving power of a grating may be expressed as  $mN$ , where  $m$  is the order of the spectrum and  $N$  is the number of grooves or rulings on the grating. There are basically two types of diffraction gratings, the transmission and the reflectance types.

The final part of the spectrometer is the detector. The IR detector is a device that measures the IR energy of the source that has passed through the spectrometer. Their basic function is to change radiation energy into electrical energy, which can be generated to process a spectrum.

In the case of FTIR spectroscopy the spectra are recorded in the time domain followed by computer transformation into the frequency domain, rather than directly in the frequency domain, as is done by dispersive IR spectrometers. However, in spite such procedure seems more complicated, they have been outlined above the advantages to be gained with FTIR. To record in the time domain, interference has to be used to modulate the IR signal at a detectable frequency. This is done by means of the well known Michelson interferometer, which is used to produce a new signal (interferogram) of a much lower frequency which contains the same information as the original IR signal.

In the Michelson interferometer radiation leaves the source and is split. Half is reflected to a stationary mirror and then back to the splitter. This radiation has travelled a fixed distance. The other half of the radiation from the source passes through the splitter and is reflected back by a movable mirror. Therefore, the path length of this beam is variable. The two reflected beams recombine at the splitter, and they interfere. If the movable mirror moves away from the beam splitter at a constant speed, radiation reaching the detector goes through a steady sequence of maxima and minima as the interference alternates between constructive and destructive phases. A simple sine wave interference pattern is produced. Each peak indicates mirror travel of one half the wavelength of the laser. The accuracy of this measurement system means that the IR frequency scale is accurate and precise. In the FTIR instrument, the sample is placed between the output of the interferometer and the detector. The sample absorbs radiation of particular wavelengths. Therefore, the interferogram contains the spectrum of the source minus the spectrum of the sample. An interferogram of a reference (sample cell and solvent) is needed to obtain the spectrum of the sample. After an interferogram has been collected, a

computer performs a Fast Fourier Transform, which results in a frequency domain trace (i.e. intensity vs. wavenumber) that is what one needs and knows.

The detector used in an FTIR instrument must respond quickly because intensity changes are rapid (the moving mirror moves quickly). So, pyroelectric detectors or liquid nitrogen cooled photon detectors must be used, while thermal detectors are too slow. To achieve a good signal to noise ratio, many interferograms are obtained and then averaged. This can be done in less time than it would take a dispersive instrument to record one scan.

For a basic description of the sources, monochromators, filters and detectors, one can see for example the book of Colthup et al. [141] and the references therein.

Although FTIR has a wide range of applications in SGS, in this work we have only used it to determine the catalytic conversion power of some samples by measuring the area of the C-O peak of the CO<sub>2</sub> molecule.

### **2.3.1. IR and Raman allowed vibrations**

As commented before, although IR and Raman measure the same vibrational spectrum, the obtained results are different, due to the selection rules that apply in each case. To determine the activity of a vibration in IR and Raman spectra, the selection rule must be applied to each normal vibration mode. According to quantum mechanics, the vibration is Raman active if one of the six components of the polarizability changes during the vibration. Similarly, it is IR active if one of the three components of the dipole moment ( $\mu_x$ ,  $\mu_y$ ,  $\mu_z$ ) changes during the vibration. However, changes in dipole moment or polarizability are not obvious from inspection of the normal modes of vibration when treating with non simple molecules and one has to appeal to group theory, which gives a clear-cut solution to this problem.

Therefore, the selection rule for the IR spectrum for a normal vibration whose normal coordinate is  $Q_a$  is determined by the integral:

$$[\mu]_{v',v''} = \int \psi_{v'}(Q_a) \mu \psi_{v''}(Q_a) dQ_a$$

where  $\mu$  is the dipole moment in the electronic ground state,  $\psi$  is the vibrational eigenfunction and  $v'$  and  $v''$  are the vibrational quantum numbers before and after the transition, respectively. The vibration is IR inactive if this integral is zero, i.e., all the three components (for  $\mu_x$ ,  $\mu_y$  and  $\mu_z$ ) are 0. If any of the three components does not vanish the vibration is infrared active.

Similarly, the selection rule for the Raman spectrum is determined by the integral:

$$[\alpha]_{v',v''} = \int \psi_{v'}(Q_a) \alpha \psi_{v''}(Q_a) dQ_a$$

or what is the same, by the six components in which can be resolved for the six components of the polarizability.

However, it is possible to decide whether the integrals are zero or nonzero from a consideration of symmetry, because the vibrations of interest are the fundamentals in which transitions occur from  $\nu''=0$  to  $\nu''=1$ , and  $\psi_1(Q_a)$  is invariant under any symmetry operation, whereas the symmetry of  $\psi_1(Q_a)$  is the same as that of  $Q_a$ . Therefore, the normal vibration associated with  $Q_a$  becomes IR active when at least one of the components of the dipole moments belong to the same symmetry species as  $Q_a$ , and similar conclusions are obtained for the Raman spectrum.

## 2.4. X-Ray Photoelectron Spectroscopy

X-rays are a short wavelength form of electromagnetic radiation discovered by Wilhelm Röntgen just before the turn of the century (Röntgen, 1898), but it was not until many years later that a Swedish physicist, K. Siegbahn, applied the XPS to chemical analysis. A schematic figure of an XPS analyser is shown in fig. 2.2.

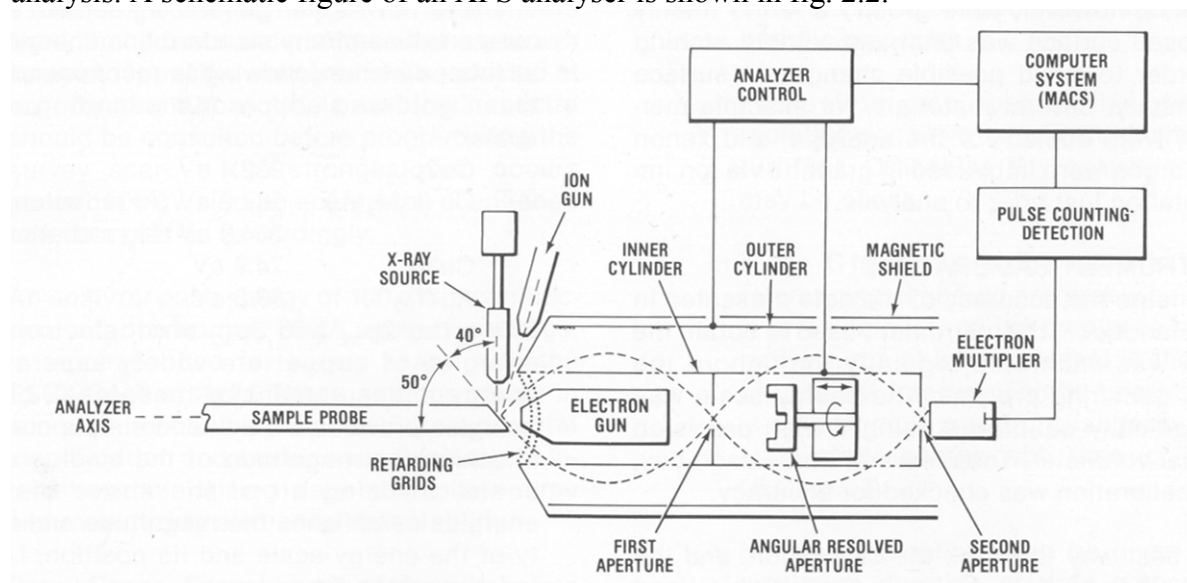


**Fig. 2.2.** Schematic representation of the PHI Model 550, ESCA/SAM system (see [149]).

In an XPS analysis, the sample is irradiated with electromagnetic radiation of energy  $h\nu$  and it emits electrons because of the photoelectric effect. These electrons have kinetic energy of the form:

$$E_{\text{kin}} = h\nu - E_B,$$

where  $E_B$  is the bond energy of the electron.

The incident radiation has energy greater than 1KeV and then the electrons come from the inner levels. The most usual source of X-Rays is a sample of Mg or Al. In it, electrons from a cathode produce ionisation of the inner levels of this element and then X-Rays are emitted.

Usually the  $K_{\alpha}$  emission is the most important and its energy in Al is 1.487 KeV with a width of 1eV and, in the case of Mg, it has energy of 1.254 KeV with a width of 0.8 eV. An XPS spectrum is obtained as a plot of the number of detected electrons per energy

interval versus their kinetic energy and the minimum width of the lines comes from the uncertainty in the radiation energy.

In order to have a reproducible analysis, the bond energies must have a reference. In gas phase the bond energy is the energy that an electron in the vacuum must receive to reach the zero potential without kinetic energy. In solids, the bond energy is the energy that we must supply to an electron to reach the Fermi level.

To have a good calibration of the lines, in metals  $E_B = 0$  in the Fermi level and this is the level with  $E_{kin}$  greater in the XPS spectrum. However, in practice, it is made fixing the position of a known line of a certain element. In insulators, the loss of electrons produces the shift of the lines to greater  $E_B$ , so the calibration is made fixing the line 1s of the C, that is part of the surface contamination.

The bond energy is proportional to  $Z^2$  (see fig. 2.3), so the measure of  $E_B$  allows the identification of the materials. Further, the XPS analysis can identify atoms of the same element with different bonds. The reason is that when the other atoms are more electronegative, the measured  $E_B$  is greater because our atom losses part of its negative charge and the internal electrons are more attracted by the core. This produces a chemical shift in the line that allows the identification of this different bonding of the element.

The XPS is essentially a surface analysis technique because we measure electrons that have no losses in their energy, then the thickness measured is of the range of  $3\lambda$ , where  $\lambda$  is the medium free length of the electron in the solid. This thickness, for energies between 100 and 1500 eV, is between 5 and 20Å.

The intensity of an XPS line is proportional to the effective section of photoelectric effect  $\theta^X$ , that accounts for the probability that a photon produces the emission of an electron in the X level. This magnitude increases when  $E_B$  increases and, for a given level, with the atomic number (fig. 2.4) and decreases when the incident radiation is more energetic.

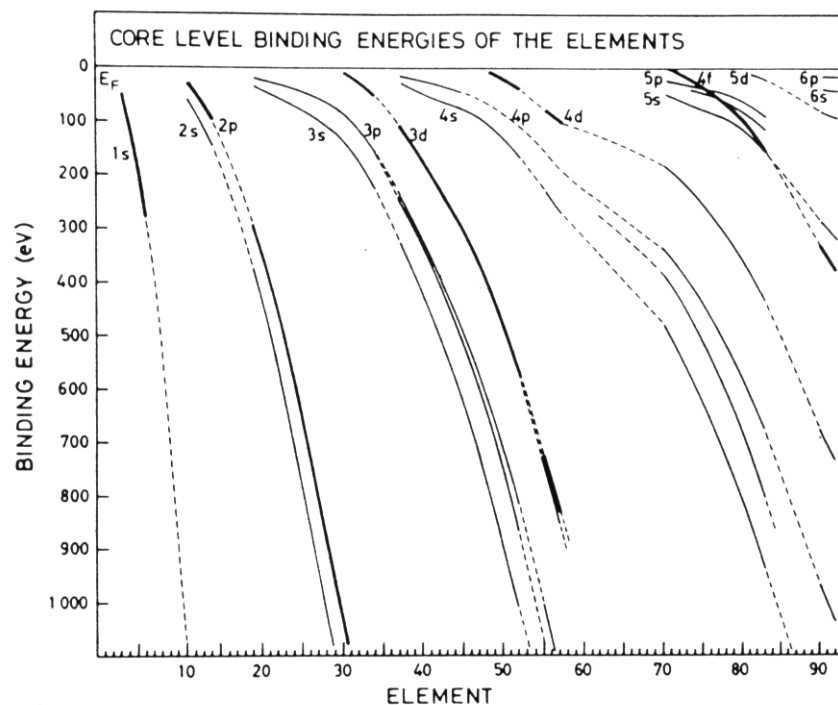


**Fig. 2.3.** Summary of all core-level energies that are accessible with Mg  $K_{\alpha}$  and Al  $K_{\alpha}$  excitation. The thick solid lines mark the narrowest levels and the dashed lines indicate either that the positions are influenced by multiplet splittings or configuration-interaction effects or that the elements are not solids in the standard state (After [148]).

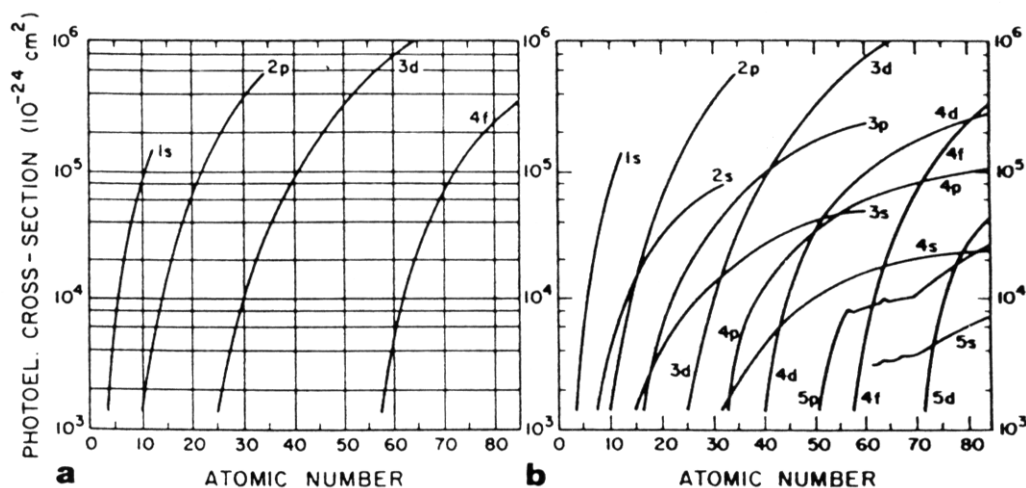


**Fig. 2.4.** Calculations of the photoelectric cross section for different subshells throughout the periodic chart. The incident radiation is 1.5 keV. (a) The dominant shells most used in XPS; (b) the complete set of subshells (see [148]).

In order to find out the concentration of an element, the areas of the lines are compared. When overlapping occurs, a deconvolution must be made. In this process each contribution receives a Gaussian or Lorentzian form.

Another important characteristic of this analysis is that the area scanned is of the order of hundreds of  $\mu\text{m}^2$ , very large when compared with those from other techniques.

Moreover, the technique induces some damage to the sample, overheating the analysed zone and destroying the local crystal structure.

## **2.5. Transmission Electron Microscopy**

In 1925-27, Busch discovered that a rotationally symmetric, inhomogeneous magnetic field could be conceived of as a lens for an electron beam. The use of electron beams for producing enlarged images was first carried out in 1932 by Ernst Ruska and Max Knoll and perfected microscopes could be mass-produced from the beginning of the 1950s. A simplified scheme of a TEM is shown in fig. 2.5.

One of the greatest advantages of the TEM is the excellent horizontal resolution (i.e., the horizontal distance of two object details just separable from one another), because it depends on the wavelength of the radiation employed, i.e., the smaller the wavelength the greater the resolution. In TEM the incident radiation is a beam of electrons that has a wavelength of the form:

$$\lambda(nm) \cong \sqrt{\frac{1.5}{V}}$$

where V is the acceleration voltage (in volts) applied to incident electrons.

The interaction between the incident beam and the sample is not only superficial, but in a certain volume of the sample. This volume is greater at greater acceleration potentials but is smaller at greater average atomic number of the sample.

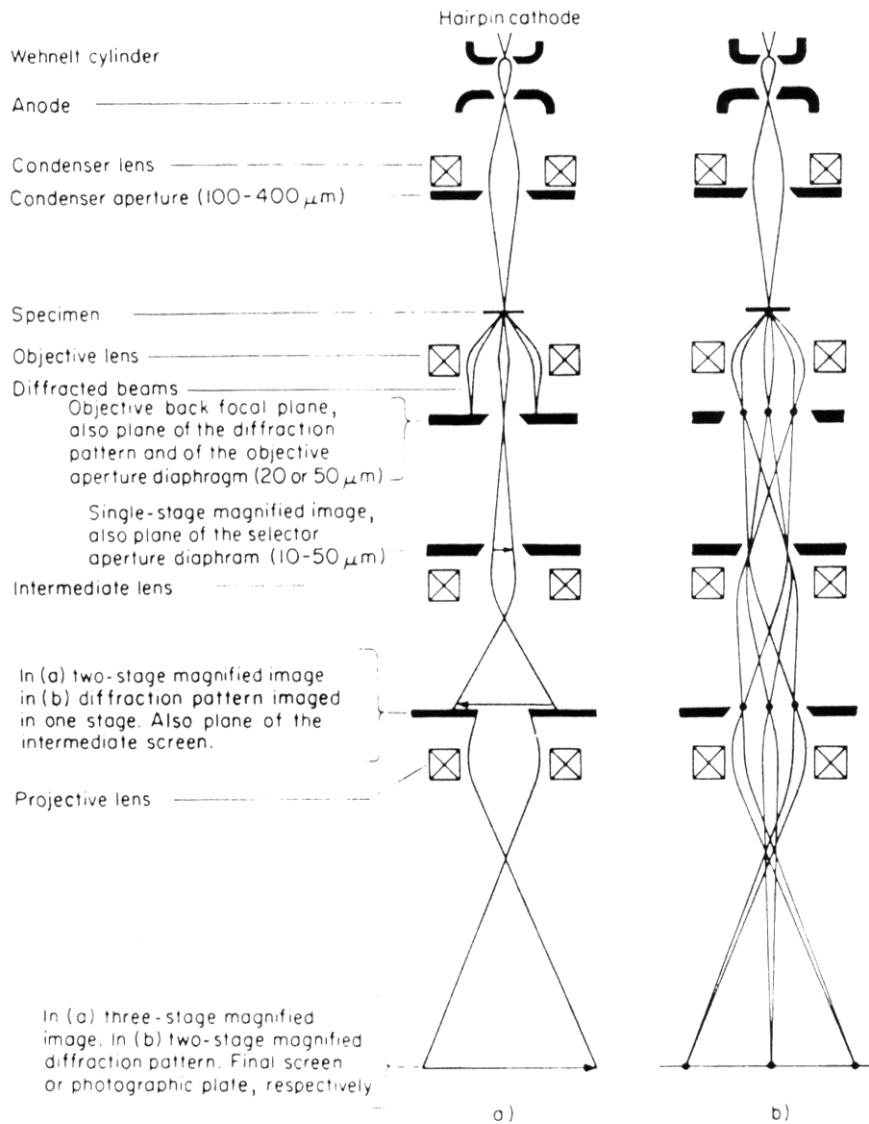


**Fig. 2.5.** Schematic design of a transmission electron microscope. A) Ray path for bright field imaging (three-stage magnification); b) Ray path for selected area diffraction (SAD). The excitation of the intermediate lens is weaker in b) than in a): thus, the primary diffraction pattern is imaged by the intermediate lens instead of the first-stage image (After [152]).

There is a great variety of TEM depending on its specific characteristics. We will briefly describe:

- CTEM (Conventional TEM) detects only the transmitted electrons.
- HRTEM (High Resolution TEM) can detect electrons diffracted at a wide range of angles.

These microscopes can also have a chemical detector in order to identify the elements that are part of the sample.



## CTEM

This is the most elemental TEM and its principles can also be extended to the other kinds of TEM.

One of the characteristics of the sample in order to provide a TEM image is that it must be very thin because the electrons detected are those which cross the sample.

There are three basic parts in a TEM:

- 1) The gun, that is at the top of the microscope. It generates the accelerated electron beam.
- 2) The vertical column, where the beam interacts with the sample and the first images are formed.
- 3) The screen, where the final image is formed.

In the gun, the beams can be produced by three ways:

- 1) Thermal emission, where a filament is heated and emits electrons because of the Joule effect. This is the most usual method in CTEM.
- 2) Indirect heating, where monocrystals of LaB<sub>6</sub> or WZr are used as filaments.
- 3) By field emission, where monocrystals of W with V-shape are used.

The two last modes are the most usual in HRTEM because they give a greater intensity and it increases the resolution.

After the generation of the beam, it is accelerated by means of a voltage applied between the filament (that acts as a cathode) and an anode.

In its column, the TEM uses electromagnetic lenses to focus the beam and resolve the image. These lenses generate an intense magnetic field that acts as a thin convex lens. The electromagnetic lenses invert the image (as the classical ones) but also rotate it.

One important problem in order to obtain the best possible resolution is the aberrations of the lenses. They can be spherical or chromatic.

The chromatic aberration comes from the different refractive indices because of the distinct wavelengths of the transmitted electrons (they have different energies depending on the part of the sample through which they have crossed) but it is avoided working with thin samples.

The spherical aberration is produced because the length travelled by the electrons across the lens depends on the electron position in the beam, i.e. the focal length of the outer lens zone is smaller than that of the inner zone. To reduce its effect, the aperture angle must be kept as small as possible but, in practice, the spherical aberration determines the attainable resolution because it cannot be compensated for by dispersion lenses as in light optics and, besides, good resolution requires an aperture angle as large as possible.

The contrast of the images in these microscopes comes from the fact that the transmitted electrons are scattered at certain angles when they cross the sample. Then, there are parts of the image that are darker because they scatter the transmitted electrons at greater angles. This working mode is called “Bright Field” because, in the absence of sample, the image is bright.

Another kind of contrast is when we collect the transmitted electrons with a certain angle (not parallel to the incident beam, as in bright field). Then, the brighter parts are those which diffract with this angle. Without sample there is a completely dark image, so this is called “Dark Field”.

Generally, the more electrons are lost by scattering when:

- the larger the atomic number of the sample.
- the larger the sample thickness to be penetrated.
- the more atoms are present for interaction in the specimen film (i.e., the greater the density).
- the smaller the aperture angle.
- the smaller the energy of the electrons.

The TEM can also collect the diffraction image of the sample, allowing better characterisation of the elements.

Of course, this microscope needs an excellent vacuum system in order to prevent crashing between the electrons of the beam and the atoms of the air gases.

In general, all the techniques used in this work (except SPM) give us excellent results when analysing the general chemical composition and structure of materials, but the results are usually integrated from the information coming from a wide area, containing a high number of particles and grains. If we want to analyse the material at the atomic scale, obtaining the nanoscopic features of composition and structure (which is crucial in SGS), TEM studies of the samples are needed.

## **2.6. Induced Coupled Plasma-Optical Emission Spectroscopy**

Flames and electrical discharges have been an important part of chemical analysis for a long time. In 1752, Thomas Melville wrote of his observations of a bright yellow light emitted from a flame produced by burning a mixture of alcohol and sea salt. One of the first uses of sparks for chemical analysis was reported in 1776 by Alessandro Volta, who discovered a way to produce a static electric charge strong enough to create sparks.

In Atomic Spectrometry techniques (that involve electromagnetic radiation), quantitative information (concentration) is related to the amount of electromagnetic radiation that is emitted or absorbed while qualitative information (what elements are present) is related to the wavelengths at which the radiation is absorbed or emitted. Every element has its own characteristic set of energy levels and thus its own unique set of absorption and emission wavelengths.

In these techniques, the sample is decomposed by intense heat into a cloud of hot gases containing free atoms and ions of the element of interest. In optical emission spectrometry (OES) the sample is subjected to temperatures high enough to cause not only dissociation into atoms but to cause significant amounts of collisional excitation (and ionisation) of the sample atoms to take place. Once the atoms or ions are in their excited states, they can decay to lower states through thermal or radiative (emission) energy transitions. Thus, the intensity of the light emitted at specific wavelengths is measured and used to determine the concentrations of the elements of interest. One of the most important advantages of OES results from the excitation properties of the high temperature sources used in OES, because they can populate a large number of energy levels that can emit, and this results in the flexibility to choose from several different emission wavelengths for an element and in the ability to measure emission from several different elements concurrently.

In general, there are three types of thermal sources normally used in analytical atomic spectrometry to dissociate sample molecules into free atoms: flames, furnaces and electrical discharges. The first two types are hot enough to dissociate most types of molecules into free atoms. The main exceptions are refractory carbides and oxides, which can exist as molecules at the upper flame and furnace temperatures of 3000-4000 K. Electrical discharges are used as atomisation sources in OES. The electrical discharges are created by applied currents or potentials across an electrode in an inert gas and typically produce higher temperatures than traditional flame systems. Most recently, other types of discharges, namely plasmas, have been used as atomisation/excitation sources for OES. Strictly speaking, a plasma is any form of matter that contains an appreciable fraction (>1%) of electrons and positive ions in addition to neutral atoms, radicals and molecules. Two characteristics of plasmas are that they can conduct electricity and are affected by a magnetic field. The electrical plasmas used for OES are highly energetic, ionised gases that are usually produced in inert gases. The Argon-supported ICP is the one used actually and it is very similar to the one described by Velmer Fassel in the early 1970's. In it, argon gas is directed through a torch consisting of three concentric tubes made of quartz or some other suitable material. A copper coil (called the load coil) surrounds the top end of the torch and is connected to a radio frequency (RF) generator. During operation, the load coil is cooled by water or gas. When RF power (typically 700-1500 Watts) is applied to the load coil, an alternating current moves back and forth within the coil, or oscillates, at a rate corresponding to the frequency of the generator. In most ICP instruments this frequency is either 27 or 40 MHz. This RF oscillation of the current in the coil causes RF electric and magnetic fields to be set up in the area at the top of the torch. With argon gas being swirled through the torch, a spark is applied to the gas causing some electrons to be stripped from their argon atoms. These electrons are then caught up in the magnetic field and accelerated by them. Adding energy to the electrons by the use of a coil in this manner is known as inductive coupling. These high-energy electrons in turn collide with other argon atoms, stripping off still more electrons. This collisional ionisation of the argon gas continues in a chain reaction, breaking down the gas into a plasma consisting of argon atoms, electrons and argon ions, forming what is known as an ICP discharge. The ICP discharge is then sustained within the torch and load coil as RF energy is continually transferred to it through the inductive coupling process. The ICP discharge appears as a very intense, brilliant white teardrop-shaped discharge. Allowing the sample to be introduced into the centre of the plasma gives the ICP many of its unique analytical capabilities, as a long residence time of the sample in the centre of the plasma is desired to eliminate matrix interferences and to ionise elements with high ionisation potentials.

Most samples begin as liquids that are nebulized into an aerosol, a very fine mist of sample droplets, in order to be introduced into the ICP. The aerosol is then carried into the centre of the plasma by an argon flow. The first function of the high temperature plasma is to remove the solvent from the aerosol, usually leaving the sample as microscopic salt particles. The next steps involve decomposing the salt particles into a gas of individual molecules (vaporisation) that are then dissociated into atoms (atomisation). Afterwards, the sample is excited and ionised. The gas temperature in the centre of the ICP is about 8000 K (see fig. 2.6), so high as to reduce or eliminate many of the chemical interferences found in flames and furnaces.

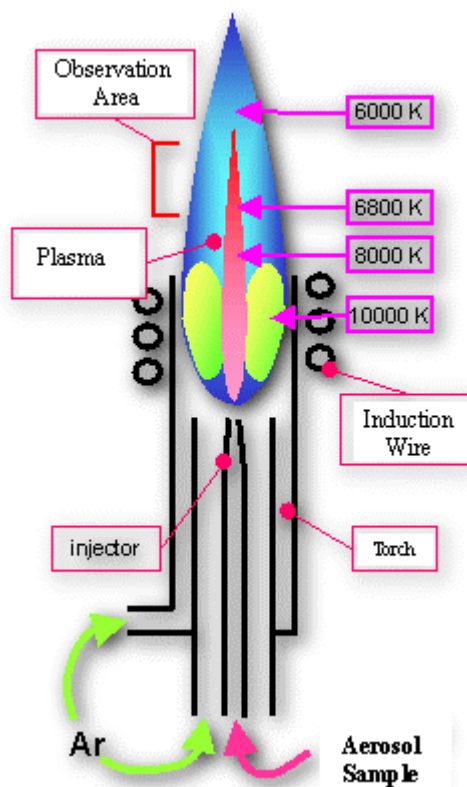


**Fig. 2.6.** Schematic representation of an ICP plasma torch.

In ICP, because the excited species emit light at several different wavelengths, it is polychromatic and is separated into individual wavelengths, that are detected using a photosensitive detector such as a photo-multiplier tube (PMT) or advanced detector techniques such as a charge-injection device (CID) or a charge-coupled device (CCD). A schematic representation of an ICP-OES instrument is shown in fig. 2.7.

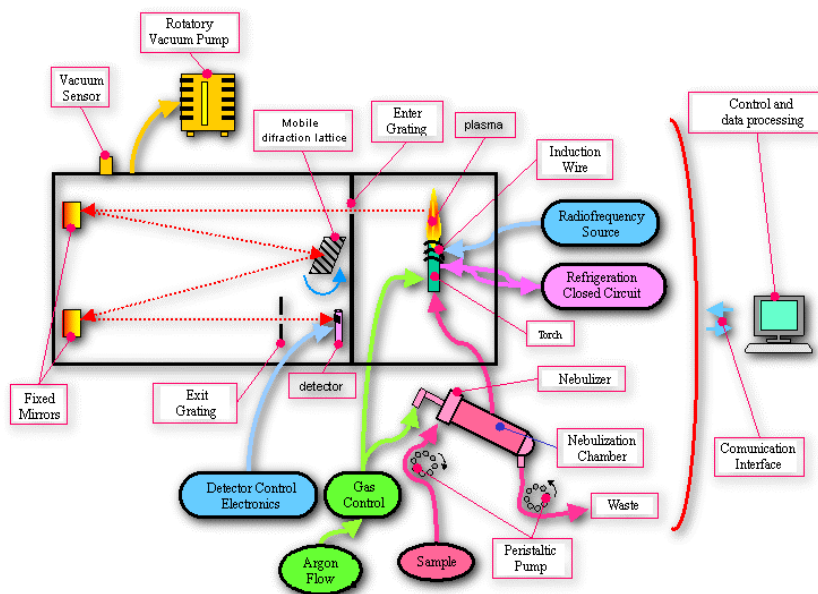


**Fig.2.7.** Schematic representation of an ICP-OES instrument.

Thus, in real samples, ICP-OES has been shown to be less susceptible to interferences than almost any other comparable spectrometric technique. The interferences that have been reported in the literature may be categorised as: 1) spectral overlap (including continuum or background radiation). It can often be eliminated by simply increasing the resolution of the spectrometer or by changing the analysed spectral line. Background continuum interference is caused by recombination radiation, that is emitted when free electrons in the plasma which have a continuous energy distribution are captured by an ion. As a result, a radiation continuum is emitted; 2) stray light interferences, that are reduced by using motorised entrance slits with polichromators and holographic gratings; 3) Absorption interferences, that arise when part of the emission of an analyte is absorbed before it reaches the detector; 4) matrix effect interferences. A significant contribution to them is made by changes that can occur in the nebulization or sample introduction. For example, changes in the acid concentration or dissolved solid content from one solution to another will alter the efficiency of nebulization and hence the sensitivity. Matrix effect from some acids (as sulphuric) are more severe than others, and dilute solutions of hydrochloric, nitric or perchloric acids are preferable.

One way to correct matrix interferences is internal standardisation, i.e., the potential for calibration with synthetic standards, that is a major advantage of ICP-OES, as it avoids the need to use chemically analysed secondary solid standards. Internal standardisation is commonly used in a genuine effort to improve performance at high concentration levels. Normally, the internal standard element is introduced at some stage of the dissolution procedure. Although no universal choice of internal standard can be made, an internal standard must satisfy the following conditions: (i) The internal standard element should not be present in the samples; (ii) Chemical compatibility with the sample must be maintained; (iii) Spectral interferences should not be significant on the internal standard line, as the internal standard concentration is usually quite low.

The nebulization process is one of the critical steps in ICP-OES. Usual commercial ICP nebulizers are pneumatic and use high speed gas flows to create an aerosol, but the transport efficiency is poor, and much research is done in this field. Nevertheless, routine



The great advantage of these techniques when compared with the techniques that collect information using a radiation is that, in the latter, the resolution is limited because features smaller than the wavelength of the radiation employed blur and cannot be resolved, but when a small probe is placed very close to a surface, the resolution is intrinsically limited by the quality of the probe: the sharper the probe, the tinier the interaction area of the surface and thus the higher the resolution.

These techniques give information only about the surface of the solid and, because of the small distance between the probe and the sample, the latter must be relatively flat and, of course, the system must have an excellent vibration insulator to prevent the crash between the tip and the sample. Besides, they lack on chemical specificity: it gives the patterns of the surfaces but it cannot resolve what kinds of elements are present.

### **2.7.1. Atomic Force Microscopy**

The AFM was designed by G. Binnig in 1986 [161]. It measures the force interaction between a sharp tip and the surface and, since the force interaction does not depend on electrically conducting samples and tips, AFM can be applied to insulators as well.

In order to measure these forces, a probe tip is mounted on a cantilever-type spring. Then, the force interaction between the sample and the tip after approaching each other causes the cantilever to deflect according to Hooke's law:

$$F = c \cdot \Delta z,$$

where  $c$  is the spring constant of the tip and  $\Delta z$  is the deflection.

These deflections can be sensed by various means. One of the most common is laser beam deflection (fig. 2.9). In this optical detection method the cantilever displacement is measured by detecting the deflection of the laser beam which is reflected off the rear side of the cantilever. The direction of the reflected laser beam is detected by a position-sensitive photodiode array.

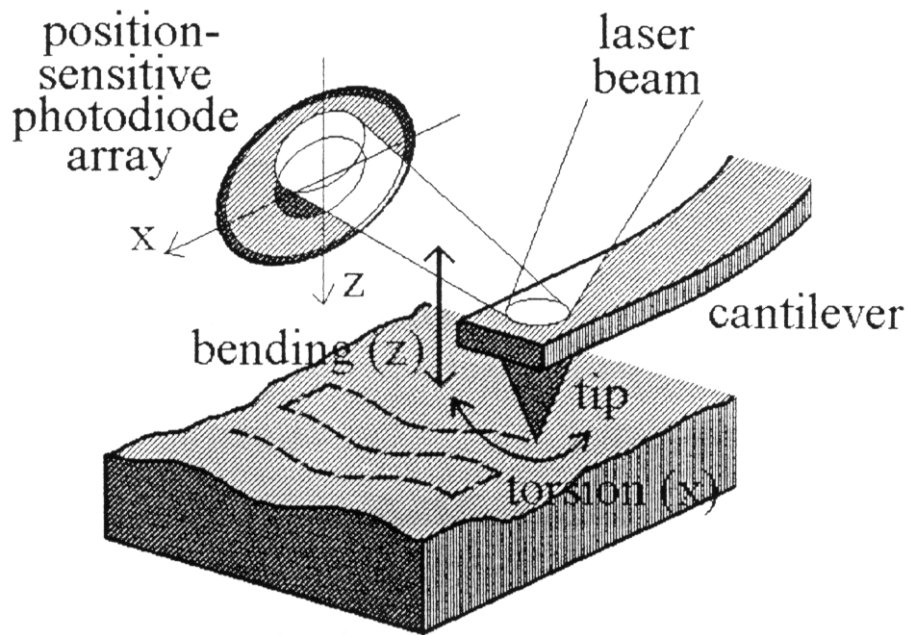


**Fig. 2.9.** Diagram showing the most common way of measuring AFM cantilever deflection (see [160]).

This detection method requires a mirror-like surface at the rear side of the cantilever. This configuration can measure separately the deflection of the cantilever due to bending and torsion forces. The former is the “force signal” used in the feedback system and thus allows imaging the surface topography, and the latter reports on friction forces.

The force sensor (cantilever and tip) of the AFM has to fulfil several requirements:

- 1) The spring constant should be small enough to allow detection of small forces.
- 2) The resonant frequency should be high to minimise sensitivity to mechanical vibrations. It allows also for reasonably high scan speeds.
- 3) For atomic resolution studies, sharp tips with small effective radius of curvature are required.

In order to increase the resonant frequency of the cantilever, its mass must be reduced. Therefore, most AFM cantilevers are microfabricated from silicon oxide, silicon nitride or pure silicon using photolithographic techniques.

The V-shaped cantilevers have an increased lateral stiffness when compared with rectangular cantilevers, leading to reduced sensitivity to lateral (frictional) forces which can cause appreciable lateral bending of the cantilever. This lateral bending can result in serious degradation of the AFM images. On the other hand, the lateral forces can also be measured and can provide useful information about the surface structure.

The force experienced by the tip when it is slowly approached to the sample surface can be plotted as in fig. 2.10. The cantilever is bent backwards in the “repulsive



force” region (a), which corresponds to a situation of contact. The cantilever is bent towards the sample in the “attractive force” region (b), in a situation of non-contact.

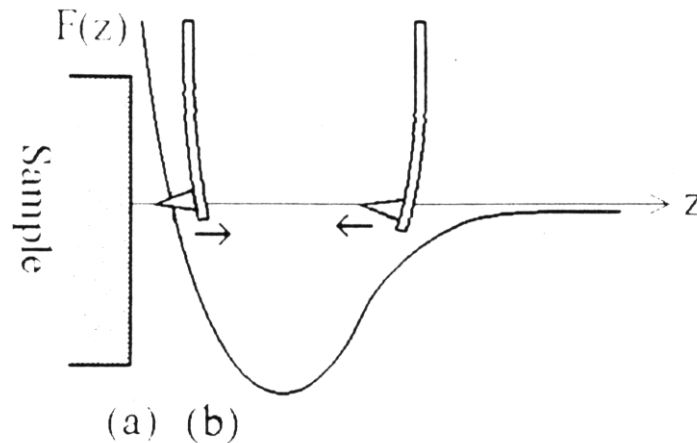


**Fig. 2.10.** Force experimented by the tip in the approach to the sample (After [160]).

When the tip and the sample are in contact, the repulsive forces arise from the short-range repulsion between the electron clouds of their atoms. In non-contact the attractive interaction is due to weaker but longer-range forces as van der Waals and electrostatic.

Since the interaction between the tip and the sample is different in these two regions, the AFM can operate in “repulsive or contact mode” or in “attractive or non-contact mode”. There is also the possibility to work in what is called “Tapping Mode”. As the images presented in this work were acquired using contact AFM in air, we will briefly describe it.

### 2.7.1.1. Contact AFM

In this mode, after bringing the tip to contact with the sample surface at a certain value of the force, the force is kept constant by a feedback system that retracts the tip when the measured force is above the set value, and approaches it when the force falls to a lower value. Two feedback modes can be distinguished and they yield different AFM images:

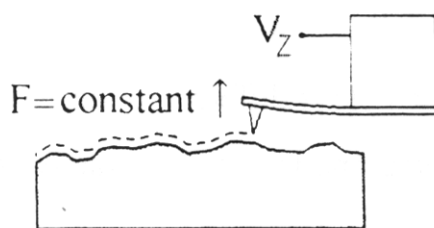


**Fig. 2.11.** AFM tip scanning a surface at constant force (see [160]).

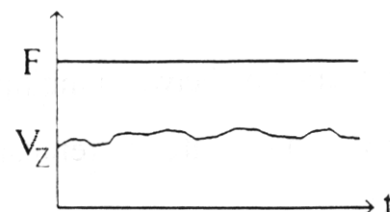


**Fig. 2.12.** Plots corresponding to fig. 2.11. (After [160]).

When the feedback system is responding fast to small changes in the applied force while the tip is scanned over the surface, then the  $z$  position of the tip is adjusted at each point to keep the force constant. In this case, the voltage  $V_z$  (i.e., the voltage applied to the piezoelectric) carries true topographic information and this imaging mode is called “Topographic, Constant Force or Constant Deflection Mode” (figs. 2.11 and 2.12)

When the feedback system is responding slowly, only the average force (and height) will be kept constant, and the features of the surface will cause variations on the force about its set value. In this mode, called “Variable Force Mode” or simply “Force Mode”, there is no height information available and the force is displayed directly (figs. 2.13 and 2.14)

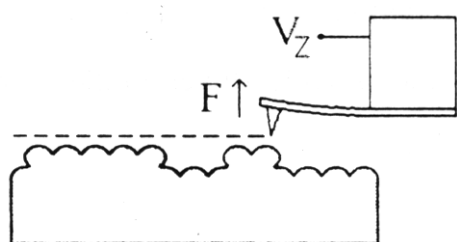


**Fig. 2.13.** *AFM tip scanning a surface at a constant height (see [160]).*

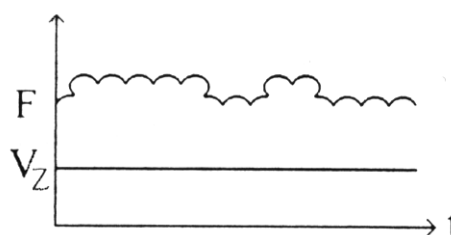


**Fig. 2.14.** *Plots corresponding to fig. 2.13. (After [160]).*

### **2.7.2. Scanning Tunneling Microscopy**

This microscope was the first member of this family. It appeared in 1982, invented by G. Binnig and H. Rohrer [162]. It uses a sharp conducting tip electrically biased with respect to the sample, which must be conductive too.

The magnitude measured by an STM is the current between the tip and the sample induced by the bias voltage, but since they are separated by a ‘gap’ of a few angstroms, electrons must ‘skip’ between them in a tunnelling process. In other words, the tip and the sample are brought to a very close proximity so that the overlap of their surrounding electron clouds becomes substantial and a tunnelling current in the order of nA can be measured, for applied voltages in the order of mV. Moreover, as the tunnelling current through the gap is exponentially dependent on the separation between the tip and the sample, the resolution is extremely good.

In order to prevent both the crashing of the tip with the sample and the dropping of the current to non-measurable values when the tip is too far, there is a simple feedback circuit that actuates on a tip-positioning device made by piezoelectric positioners.

The technique used in this work, EC-STM, is a modern variation of STM. The main difference is that in EC-STM there is an additional bipotentiostat that allows to control the voltage applied to the sample, that is immersed in a liquid, thereby allowing the atomic imaging of processes under electrochemical control (see fig. 2.15).

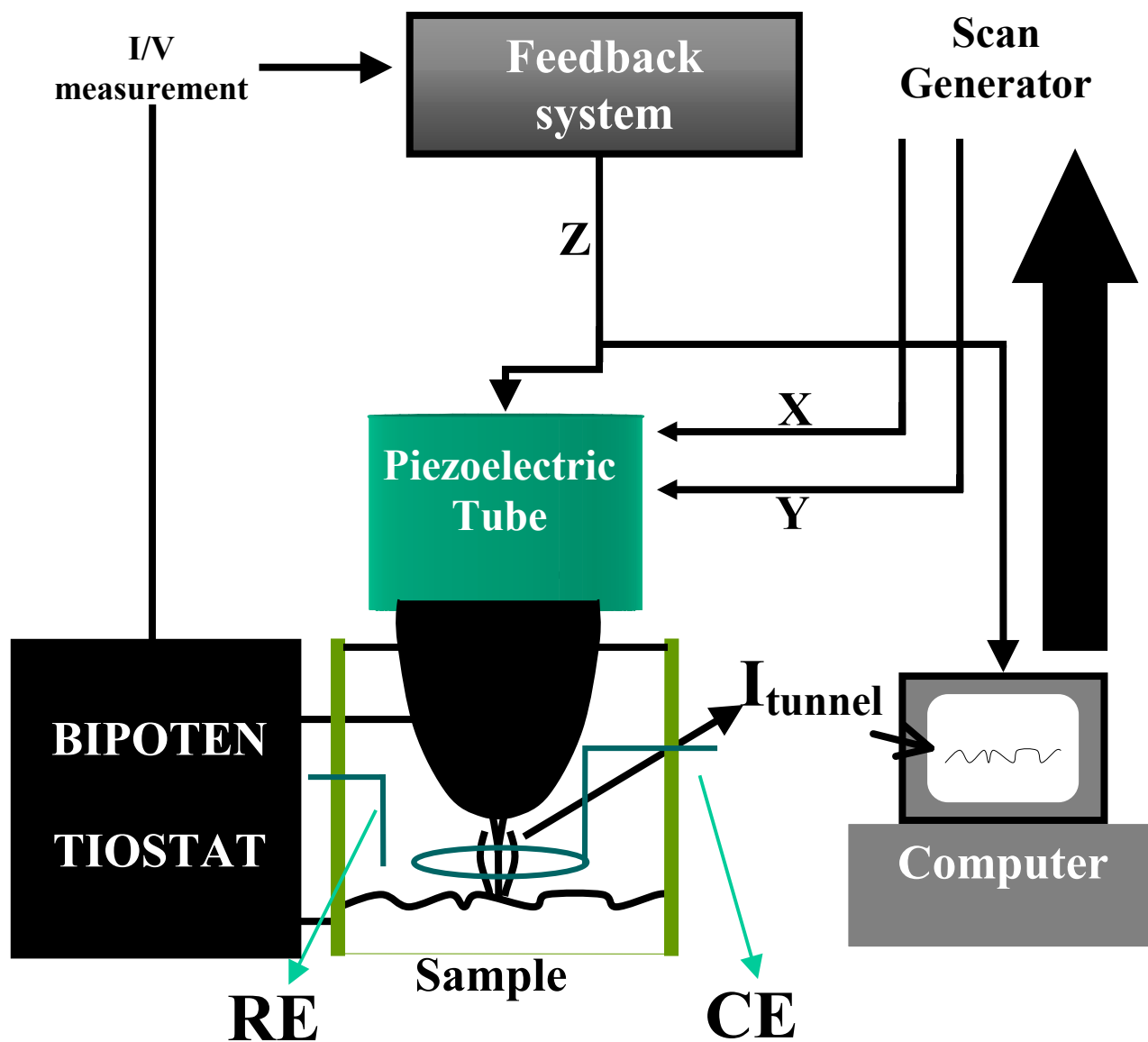
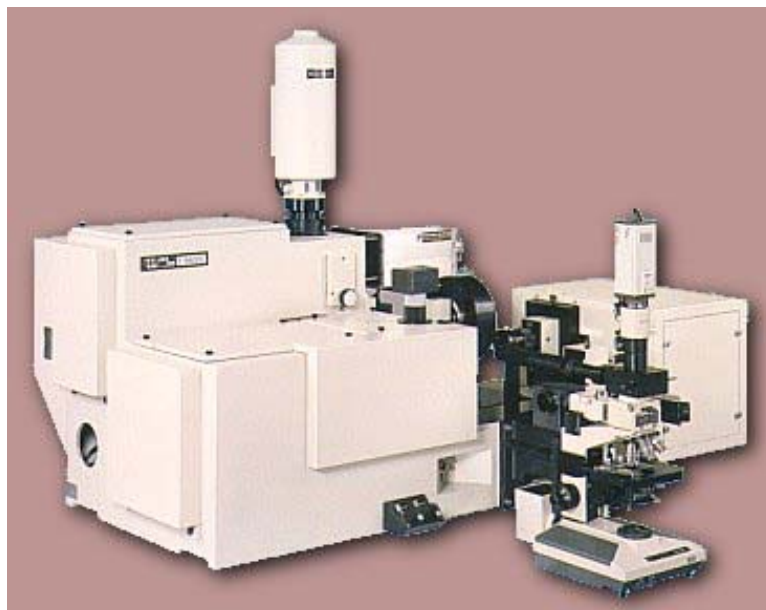


Fig. 2.15. Scheme of an EC-STM instrument.

## 2.8. Instrumentation used in this work

X-ray diffraction (XRD) patterns have been obtained with a Siemens D-500 X-ray diffractometer using Cu  $K_{\alpha}$  radiation ( $\lambda = 1.5418 \text{ \AA}$ ), with an operating voltage of 40 kV and a current of 30 mA. Data were collected in steps of  $0.05^{\circ}$  ( $2\theta$ ) from  $20$  to  $80^{\circ}$ .



**Fig. 2.16.** *Image of the Jobin Yvon T64000 Raman spectrometer.*

A Jobin Yvon T64000 Raman spectrometer (fig. 2.16) with an INNOVA 300 Coherent Ar laser, triple monochromator (1800 g/mm), bidimensional CCD detector cooled with liquid nitrogen and an Olympus BH2 microscope (50x objective) was used for Raman analysis.

X-Ray Photoelectron Spectroscopy (XPS) data were collected in a Physical Electronics 5500 spectrometer (fig. 2.17), working at a vacuum pressure of  $6 \cdot 10^{-9}$  Torr. Aluminium  $K_{\alpha}$  X-ray source, which produces photons with an energy of 1486.6 eV and a natural line width of 0.9 eV was used.



**Fig. 2.17.** *Image of a Physical Electronics 5500 spectrometer.*

Transmission Electron Microscopy (TEM) was carried out on a Phillips CM30 SuperTwin electron microscope operated at 300 keV with 0.19 nm point resolution. For TEM observations, SnO<sub>2</sub> nanopowders were ultrasonically dispersed in ethanol and deposited on amorphous carbon membranes. Image processing was made using DigitalMicrograph and Photoshop software.



**Fig. 2.18.** *Image of a Perkin-Elmer Optima 3200 RL spectrometer.*

A Perkin-Elmer Optima 3200 RL spectrometer (fig. 2.18) was used for the Induced Coupled Plasma-Optical Emission Spectroscopy (ICP-OES) measurements. It has a radiofrequency source of 40MHz, with a working power between 750 and 1500 W and a SCD detector with simultaneous measure of 235 subarrays.

For the FTIR measures, we have used a Bomem MB-120 FTIR Spectrometer (fig. 2.19). Its working range is from 350 to 5000 cm<sup>-1</sup>, with a maximum resolution of 1 cm<sup>-1</sup>. This machine has a DTGS detector, a Glowbar source and KBr as beam splitter. We have used a gas cell accessory that, together with a Nitrogen purge, allowed us to control the ambient gas.

For the AFM images, a Digital Instruments (fig. 2.20) equipment consisting in a Nanoscope IIIa Digital Instruments (Santa Barbara, CA) controller and a Molecular Imaging (Phoenix, Arizona) head was used. The AFM scanner has 7 μm of range and the tips were made of SiN, with triangular geometry. They have a spring constant of 0.1 N/m.



**Fig. 2.19.** Image of a Bomem MB-120 FTIR Spectrometer.

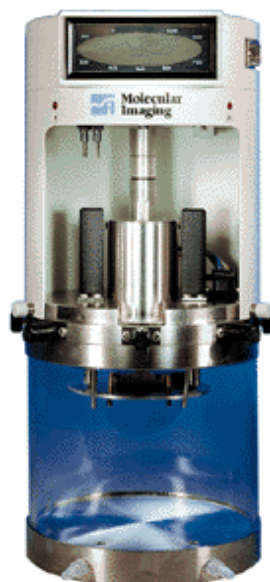


**Fig. 2.20.** Image of the Digital Instruments used to acquire the AFM images.

An optical interferometric microscope was used for the study of the roughness of different samples. The equipment used was a ZYGO model GPIxp (Zygo Corporation, Connecticut) (fig.2.21), which can have a lateral resolution of 500 nm and an axial resolution of 0.1 nm (with a maximum range of 100  $\mu\text{m}$  in Z). In table 1 the most important parameters of the objectives used are summarised.

Objective	Lateral resolution ( $\mu\text{m}$ )	Maximum sweep area ( $\mu\text{m}^2$ )
5x	3.6	1470 x 1100
40x	0.73	183 x 137

**Table 1.** Parameters attained with Zygo GPIxp.



**Fig. 2.21.** Image of a ZYGO model GPIxp.

For the electrochemical studies, either a manual potentiostat (HQ instruments 105) connected to a signal generator (EG&G Universal Programmer 175) and an analog plotter (Philips PM 8033) or a digital electrochemistry equipment “SOLARTRON SI 1287 Electrochemical Interface” was used. It has a resolution of  $1 \mu\text{V}$  in voltage and  $1 \text{ pA}$  in current, with maximum ranges of  $\pm 14.5 \text{ V}$  and  $\pm 2 \text{ A}$  respectively. It has an Electrochemistry/Corrosion software (CorrWare v1.2), commonly used elsewhere (SOLARTRON, Farnborough, England). The capacitance measurements were performed with a frequency response analyser (Solartron 1255). The Reference Electrode was a SCE from Metrohm. A scheme is shown in fig. 2.22.

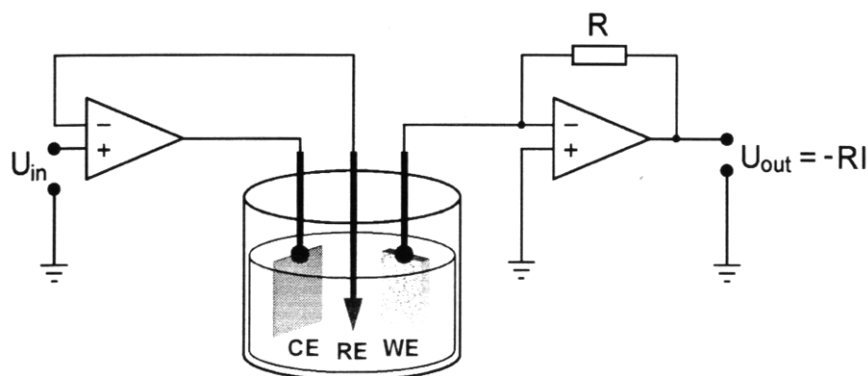


**Fig. 2.22.** Schematic representation of a potentiostat in “three-electrode” configuration (After [129]).